ELECTRONIC SUPPORTING INFORMATION

For

Heteroscorpionate Aluminium Complexes as Chiral Building Blocks to Engineer Helical Architectures.

Jose A. Castro-Osma,[a] Carlos Alonso-Moreno,[b] M. Victoria Gómez,[a] Isabel Márquez-Segovia,[a] Antonio Otero,*[a] Agustín Lara-Sánchez,*[a] Juan Fernández-Baeza,[a] Luis F. Sánchez-Barba,[a] Ana M. Rodríguez.[a]

[a]*Departamento de Química Inorgánica, Orgánica y Bioquímica, Facultad de Ciencias y Tecnologías Químicas, Universidad de Castilla-La Mancha, 13071-Ciudad Real, Spain*

[b]*Departamento de Química Inorgánica, Orgánica y Bioquímica, Facultad de Farmacia, Universidad de Castilla-La Mancha, 02071-Albacete, Spain*

E-mail: Antonio.Otero@uclm.es

Table of Contents

1. Diffusion NMR measurements

Diffusion (PFGSE) experiments were performed at 298 K using the DOSY bipolar pulse pair stimulated echo with convention compensation (Dbppste_cc in the Varian DOSY package) sequence for the determination of the self-diffusion of complex **2** at different concentrations, with 11 increments in the gradient strength, typically 64 averages per increment step (except 1024 averages per increment step for the 10mM sample concentration), and the duration of the magnetic field pulse gradient (δ) and the diffusion times (Δ) optimized for each sample as the gradient strength (G) increases to obtain 70% attenuation of the signal. Two different NMR experiments were performed on each sample, focusing on both the attenuation of the TMS signal (30% of signal remaining) and the same level of attenuation for the complex signal (30% of signal remaining). The same level of attenuation (30%) and the same gradient strength range (3000, 25000) were used for the calibration of the gradient strength. The Doneshot pulse sequence was used for the gradient calibration by means of the diffusion of HDO in D_2O at 25 ºC. For complex **2**, δ and Δ values depend on the concentration in order to reach 70% of the attenuation for all cases. To reach 70% attenuation of the TMS signal, 1 ms was used for the duration of the pulse gradient and 50 ms for the diffusion time. Pseudo-2D DOSY plots were processed with the DOSY Toolbox5 (http://personalpages.manchester.ac.uk/staff/mathias.nilsson/software.htm) with reference deconvolution (using the TMS signal) performed to correct for systematic errors.

2. Calculation of the solution viscosity, hydrodynamic radius and hydrodynamic volume

Calculation of the solution viscosity (η)

The modified Stokes–Einstein equation (3), which combines equations (1) and (2) is used to obtain an accurate estimation of r_H for medium- and small-sized molecules when the diffusion coeficient is obtained from PFGSE NMR experiments. These equations take into account the relative solute/solvent size [c (r_{solv}, r_H)] and the shape of the molecules [$f_{(a,b)}$] as an improvement of the original Stokes–Einstein equation.[1]

$$D_t = KT \,/\, c \,(r_{solv}, r_H) \, fs \,(a,b) \, 6 \, \pi\eta rH \qquad (1)$$

$$c = 6/[1 + 0.695 \,(r_{solv}/r_H)^{2.234}] \qquad (2)$$

$$D_t = KT \,[1 + 0.695 \,(r_{solv}/r_H)^{2.234}] \,/\, 6\eta\pi rH \qquad (3)$$

Where K is the Boltzmann constant, T is the temperature, η is the solution viscosity, fs(a,b) is a factor for non-spherical molecules, r_H is the hydrodynamic radius of the molecule and r_{solv} is the solvent

radius.

The concentration range for our samples is not within the low mM range and, as a result, the solution viscosity can not be assumed to be the same as that of the pure solvent.[2] Several different approaches can be used to estimate the viscosity. For example, it can be calculated by considering the diffusion coefficient relative to the non-deuterated solvent residue in pure solvent and in the solution.[1c] Anomalous diffusion data were observed, giving a lower value than that expected for the non-deuterated benzene in every sample, presumably due to the fact that solvent molecules are trapped within the molecular structure. This finding ruled out the use of this first simplification.

Another approach involves the use of an internal standard (a calibrant molecule of known hydrodynamic radius)[3] assuming that the ratio of the diffusion of a particular solute (D) and the reference compound (D_{ref}) is independent of the viscosity: $D/D_{ref} = r_{Href}/r_H$. Considering that $c(r_{solv}, r_H)$ from equation 2 is related to molecular size, it is also assumed that the reference and the solute have similar sizes. In our experimental conditions, the use of this equation becomes problematic since the average dimensions of the species present in solution can easily change on varying concentration and, consequently, the standard would not be suitable for all conditions.

As a consequence, equation 3 was used to estimate solution viscosity of the medium by means of the calculated diffusion coefficient of tetramethylsilane (TMS)[4] since TMS is not expected to be involved in any kind of interaction, and therefore a constant value for its radius can be assumed. The relative small/medium size of TMS meant that equation 1 was used with a c factor value different of 6 or 4, resulting in equation 3.[1c] Computational calculations were performed with the Gaussian 09 Rev. C series of programs,[5] to estimate the hydrodynamic radius of TMS in benzene (r_H). The radius of TMS was computed on an optimized structure by means of density functional calculations at the B3LYP level of theory with the 6-31G* basic set. A radius of 3.26 Å was obtained, which does not correspond to either c = 6 or c = 4 as reported,[1c] thus confirming the need to use $c(r_{solvent}, r_H)$. In order to obtain the solution from equation 3, another factor must be calculated – namely the solvent radius (r_{solv}). This factor was experimentally calculated by measuring D (m^2/s) for a sample of pure deuterated benzene in the presence of TMS, following the decrease of the signal due to the small percentage of nondeuterated solvent as a function of the gradient strength (G) increase.[1c] The viscosity (η) value for the deuterated solvent at 298 K is known from the literature, $\eta_{(benzene-d)}$ (298 K) = 6.878×10^{-4} Pa·s. A diffusion value of 22.6×10^{-10} m^2/s was obtained for the residual proton signal of benzene. This resulted in a solvent radius of 2.53×10^{-10} m, which is consistent with values reported in the literature[1c] with an error of only ~5% with respect to the reported data. This error is considered small and is comparable to the experimental error of the measurements. This fact also illustrates the good performance of the PFGSE measurement and the correct optimization of all the experimental NMR parameters. At this point, the solution viscosity for each sample was calculated

from equation 3 when performing a ^{1}H PFGSE NMR experiment at 298 K on each sample to determine the diffusion constant of TMS, with the attenuation focused on the TMS signal.

Calculation of the hydrodynamic radius (r_H) and hydrodynamic volume (V_H). The hydrodynamic radius was extracted from equation 3 by performing concentration-dependent ^{1}H PFGSE NMR experiments at 298 K on each sample to determine the diffusion constant of complex **2**, with the attenuation focused on protons $H^{4,4'}$ of the complex, i.e. those involved in the CH−π interactions. The value considered for benzene as a solvent was calculated experimentally as explained above and is assumed to be constant. The solution viscosity value was calculated for each sample as explained previously. For the calculation of the hydrodynamic volume the supramolecular system and the single molecule are considered to be spherical.

The uncertainty in measurements was calculated by the estimation of the standard deviation of the diffusion coefficient by performing experiments with different delay between gradients, Δ. The standard deviation observed for the hydrodynamic radius was about 4–6%.

3. X-ray crystallographic structure determination

CCDC- 756898 – 933659 – 933660 – 933662 contains the supplementary crystallographic data for **2**, **6**, **8** and **16** respectively. These data can be obtained free of charge from The Cambridge Crystallographic Data Centre via. Data were collected on a Bruker X8 APEX II CCD-based diffractometer equipped with a graphite monochromated MoKα radiation source (λ = 0.71073 Å). The crystal data, data collection, structural solution and refinement parameters are summarized in Table 1. Data were integrated using SAINT[6] and an absorption correction was performed with the program SADABS.[7] The structure was solved by direct methods using the SHELXTL package[8] and was refined by full-matrix least-squares methods based on F^2. Complexes **6**, **8** and **16** show high disorder in the ethyl groups and toluene solvate and these atoms were refined with many restrictions. For **6**, the Flack parameter could not be determined due to poor diffraction. All non-hydrogen atoms were refined with anisotropic thermal parameters except those of the disordered groups and the hydrogen atoms, which were geometrically situated.

Table S1. Selected Bond Distances (Å) and Angles (deg) for compounds **2**, **6**, **8** and **16**.

2			
Bond Distances		**Angles**	
Al(1)–S(1)	2.2858(8)	N(4)–Al(1)–S(1)	94.92(6)
Al(1)–N(4)	1.970(2)	N(4)–Al(1)–C(22)	105.10(9)
Al(1)–C(20)	1.966(2)	C(22)–Al(1)–N(4)	105.10(9)
Al(1)–C(22)	1.962(2)	C(22)–Al(1)–C(20)	120.8(1)
Al(2)–N(2)	1.966(2)	N(5)–Al(2)–N(2)	94.15(8)
Al(2)–N(5)	1.891(2)	C(26)–Al(2)–N(2)	107.95(9)
Al(2)–C(24)	1.974(2)	C(26)–Al(2)–N(5)	112.3(1)
Al(2)–C(26)	1.962(2)	C(26)–Al(2)–C(22)	120.2(1)
S(1)–C(12)	1.766(2)	N(5)–C(12)–S(1)	119.4(1)
N(5)–C(12)	1.374(3)	N(5)–C(12)–C(11)	119.5(2)

6			
Bond Distances		**Angles**	
Al(1)–O(1)	1.796(5)	N(3)–Al(1)–O(1)	94.5(3)
Al(1)–N(3)	1.947(6)	N(3)–Al(1)–C(17)	112.2(7)
Al(1)–C(17)	1.96(1)	C(17)–Al(1)–C(19)	121.3(2)
Al(1)–C(19)	1.98(1)	C(19)–Al(1)–N(3)	107(1)
Al(2)–N(1)	1.965(6)	N(5)–Al(2)–N(1)	95.5(3)
Al(2)–N(5)	1.882(6)	C(21)–Al(2)–N(1)	117(1)
Al(2)–C(21)	1.94(2)	C(21)–Al(2)–N(5)	122.8(9)
Al(2)–C(23)	1.971(9)	C(23)–Al(2)–C(21)	101(1)
O(1)–C(12)	1.343(8)	N(5)–C(12)–O(1)	122.0(6)
N(5)–C(12)	1.336(8)	N(5)–C(12)–C(11)	119.9(7)
C(11)–C(12)	1.397(9)	C(11)–C(12)–O(1)	117.8(6)

8			
Bond Distances		**Angles**	
Al(1)–N(4)	1.987(3)	N(5)–Al(1)–N(4)	94.1(1)
Al(1)–N(5)	1.889(3)	N(5)–Al(1)–C(23)	112.3(1)
Al(1)–C(21)	1.966(4)	C(23)–Al(1)–N(4)	106.6(1)
Al(1)–C(23)	1.964(4)	C(23)–Al(1)–C(21)	116.6(2)
Al(2)–O(1)	1.785(3)	C(27)–Al(2)–N(2)	107.1(3)
Al(2)–N(2)	1.956(3)	C(27)–Al(2)–C(25)	125.6(4)
Al(2)–C(25)	1.951(4)	O(1)–Al(2)–N(2)	95.4(1)
Al(2)–C(27)	1.93(1)	C(25)–Al(2)–N(2)	112.0(2)
O(1)–C(12)	1.322(4)	N(5)–C(12)–O(1)	121.1(3)
N(5)–C(12)	1.352(4)	N(5)–C(12)–C(11)	119.8(3)
C(11)–C(12)	1.365(5)	C(11)–C(12)–O(1)	119.1(3)

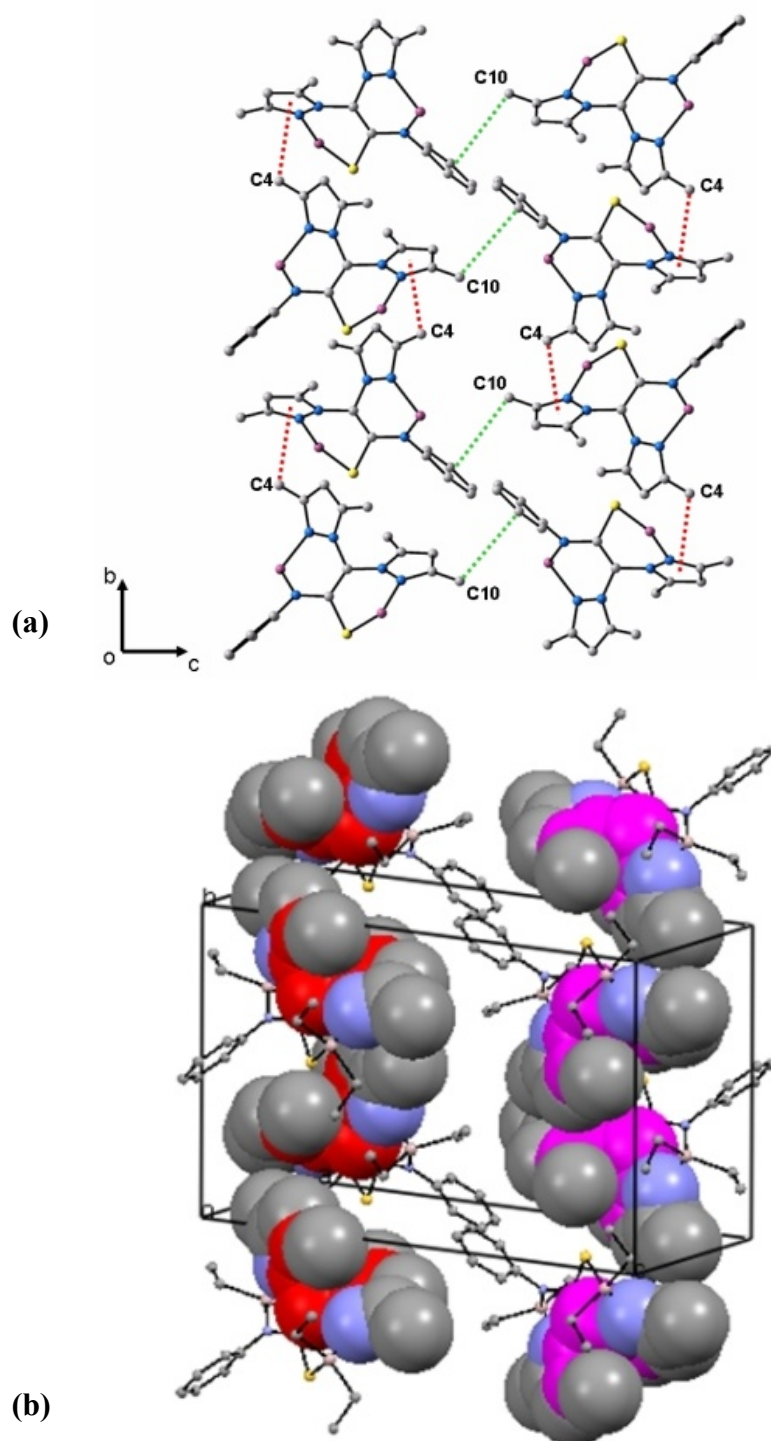| 16			
Bond Distances		**Angles**	
Al(1)–N(3)	1.970(3)	N(3)–Al(1)–C(23)	107.7(2)
Al(1)–N(5)	1.913(3)	N(5)–Al(1)–N(3)	95.9(1)
Al(1)–C(21)	1.979(4)	C(21)–Al(1)–N(5)	113.2(2)
Al(1)–C(23)	1.976(5)	C(23)–Al(1)–C(21)	118.1(2)
Al(3)–N(1)	1.972(4)	O(1)–Al(3)–N(1)	89.9(1)
Al(3)–O(1)	1.886(3)	C(31)–Al(3)–O(1)	113.5(2)
Al(3)–C(31)	1.945(6)	C(31)–Al(3)–C(33)	117.8(3)
Al(3)–C(33)	1.954(5)	C(33)–Al(3)–N(1)	114.8(2)
Al(2)–O(1)	1.985(2)	Al(3)–O(1)–Al(2)	123.7(1)
N(5)–C(12)	1.340(4)	N(5)–C(12)–O(1)	120.9(3)
O(1)–C(12)	1.383(4)	N(5)–C(12)–C(11)	124.3(3)
C(11)–C(12)	1.371(5)	C(11)–C(12)–O(1)	114.8(3)

Figure S1. (a) Ball-and-stick view (down the *b* axis) of the intermolecular interactions in complex **2**. The CH–π interactions that give rise to single-stranded helicates are marked as red dashed lines and the CH–π interactions that give rise to a sheet are marked as green dashed lines. The hydrogen atoms and the ethyl groups on aluminium atoms are omitted for clarity. (b) Space-filling view of the two adjacent *M* (left) and *P* (right) helicates for **2**.

4. Structure Determination of 1 and 13. Data were collected on a Bruker X8 APEX II CCD-based diffractometer, equipped with a graphite monochromated MoKα radiation source (λ = 0.71073 Å). Data were integrated using SAINT[6] and an absorption correction was performed with the program SADABS.[7] The structure was solved by direct methods using SHELXTL package,[8] and refined by full-matrix least-squares methods based on F^2.

The available crystals of **1** systematically exhibited poor crystallinity, which was ultimately reflected in weak diffraction intensity, especially at higher diffraction angles, and with rather broad reflections. OMIT -2 46 instruction has been used to improved the value of R indices. The crystals for **13** show decomposition during the experiment and despite several crystals are measurements, the spectra of them resulting very poor.

For **1** and **13** the squeeze utility[9] has been necessary. All non-hydrogen atoms were refined with anisotropic thermal parameters except those the disordered groups and the hydrogen atoms were geometrically situated.
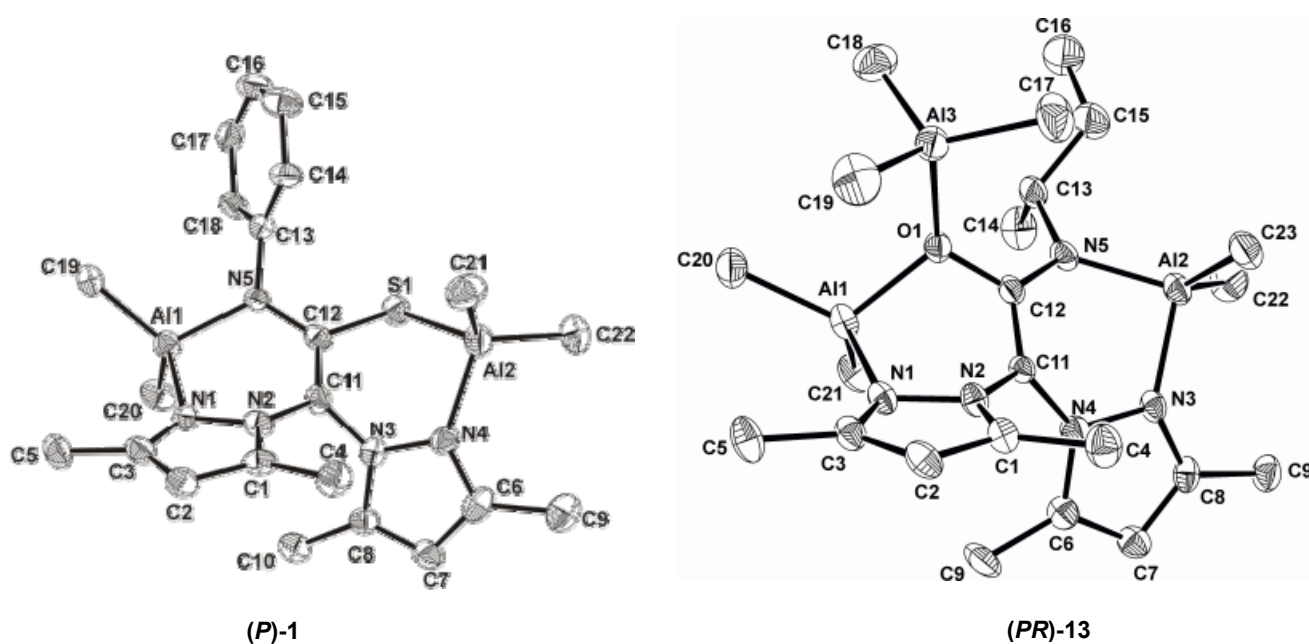

(*P*)-1   (*PR*)-13

Figure S2. ORTEP drawings of compounds **1** and **13**.

Table S2. Crystal data and structure refinement for **1** and **13**.

	1	13
Empirical formula	$C_{22} H_{31} Al_2 N_5 S$	$C_{23} H_{44} Al_3 N_5 O$
Formula weight	451.54	487.57
Temperature (K)	230(2)	230(2)
Wavelength (Å)	0.71073	0.71073
Crystal system	Monoclinic	Monoclinic
Space group	C2/c	P2$_1$/n
a(Å)	15.387(8)	9.725(8)
b(Å)	19.980(8)	34.833(5)
c(Å)	18.787(8)	10.122(9)
α(°)		
β(°)	97.84(1)	102.84(2)
γ(°)		
Volume(Å^3)	5721(4)	3343(4)
Z	8	4
Density (calculated) (g/cm^3)	1.048	0.969
Absorption coefficient (mm^{-1})	0.190	0.133
F(000)	1920	1056
Crystal size (mm^3)	0.12 x 0.11 x 0.07	0.42 x 0.38 x 0.28
Index ranges	-16≤h≤16 -21≤k≤21 -20≤l≤20	-9≤h≤5 -32≤k≤31 -9≤l≤9
Reflections collected	13309	6190
Independent reflections	3962 [R(int) = 0.1886]	2961 [R(int) = 0.0622]
Data / restr / param	3962 / 0 / 279	2961 / 0 / 304
Goodness-of-fit on F^2	0.792	0.952
Final R indices [$I>2\sigma(I)$]	R1 = 0.0774 wR2 = 0.1586	R1 = 0.0618 wR2 = 0.1471
Larg. diff. peak/hole, e.Å^{-3}	0.251 and -0.241	0.243 and -0.192

References

1 (a) R. Evans, Z. Deng, A. K. Rogerson, A. S. McLachlan, J. J. Richards, M. Nilsson, G. A. Morris, *Angew. Chem. Int. Ed.* 2013, **52**, 1-5; (b) A. Macchioni, G. Ciancaleoni, C. Zuccaccia, D. Zuccaccia, *Chem. Soc. Rev.* 2008, **37**, 479-489; (c) D. Zuccaccia, A. Macchioni, *Organometallics* 2005, **24**, 3476–3486.

2 T. D. W. Claridge, *in High-Resolution NMR Techniques in Organic Chemistry*, Vol. 27, ELSEVIER, Oxford, 2009, pp.320–329.

3 E. J. Cabrita, S. Berger, *Magn. Reson. Chem.* 2001, **39**, S142-S148.

4 C. Anselmi, F. Bernardi, M. Centini, E. Gaggelli, N. Gaggelli, D. Valensin, G. Valensin, *Chem. Phys. Lipids* 2005, **134**, 109–117.

5 Gaussian 09, Revision C.1, M. J. Frisch, G. W. Trucks, H. B. Schlegel, G. E. Scuseria, M. A. Robb, J. R. Cheeseman, G. Scalmani, V. Barone, B. Mennucci, G. A. Petersson, H. Nakatsuji, M. Caricato, X. Li, H. P. Hratchian, A. F. Izmaylov, J. Bloino, G. Zheng, J. L. Sonnenberg, M. Hada, M. Ehara, K. Toyota, R. Fukuda, J. Hasegawa, M. Ishida, Y. Nakajima, Y. Honda, O. Kitao, H. Nakai, T. Vreven, J. A. Jr. Montgomery, J. E. Peralta, F. Ogliaro, M. Bearpark, J. J. Heyd, E. Brothers, K. N. Kudin, V. N. Staroverov R. Kobayashi, J. Normand, K. Raghavachari, A. Rendell, A. J. C. Burant, S.S. Iyengar, S. J. Tomasi, M. Cossi, N. Rega, N. J. Millam, M. Klene, J. E. Knox, J. B. Cross, V. Bakken, C. Adamo, J. Jaramillo, R. Gomperts, R. E. Stratmann, O. Yazyev, O. A. J. Austin, R. Cammi, C. Pomelli, J. W. Ochterski, R. L. Martin, K. Morokuma, V. G. Zakrzewski, G. A. Voth, P. Salvador, J. J. Dannenberg, S. Dapprich, A. D. Daniels, O. Farkas, J. B. Foresman, J. V. Ortiz, J. Cioslowski, D. J. Fox, Gaussian, Inc., Wallingford CT, 2009.

6 SAINT+ NT ver. 6.04. SAX Area-Detector Integration Program. Bruker AXS 1997–2001. Madison, WI.

7 Sheldrick, G.M. SADABS version 2.03, a Program for Empirical Absorption Correction; Universität Göttingen, 1997–2001.

8 Bruker AXS SHELXTL version 6.10. Structure Determination Package. Bruker AXS 2000. Madison, WI.

9 A. L. Spek, *Acta Crystallogr.* 1990, **A46**, C-34.